IEEE Robotics and Automation Letters (RAL) paper presented at
2024 IEEE/RSJ International Conference on Intelligent Robots and Systems (IROS)
October 14-18, 2024. Abu Dhabi, UAE

Fabrication Process for Twisting Artificial Muscles by Utilizing Braiding Technology and Water-Soluble Fibers

Weihang Tian, Shuichi Wakimoto, Daisuke Yamaguchi, and Takefumi Kanda, *Member, IEEE*

***Abstract*—The McKibben artificial muscle is a pneumatic soft actuator consisting of a rubber tube, with fibers covering it. In this study, we propose a new fabrication process to easily realize twisting artificial muscles by utilizing braiding technology and water-soluble fibers based on the McKibben artificial muscle. In the braiding process, half of the sleeve fibers of the artificial muscle are substituted with water-soluble fibers. However, the water-soluble fibers are removed by placing the muscle in warm water to realize a twisting motion. By changing the direction of the fibers, artificial muscles that twist clockwise or counterclockwise can be produced. We believe that the establishment of such a simple and efficient fabrication process will promote to the practical application of artificial muscles.**

***Index Terms*—Soft robot materials and design, hydraulic/pneumatic actuators, soft robotics, artificial muscles.**

I. Introduction

ROBOTS are generally composed of rigid components and actuators; over the years, they have constantly evolved to realize "controllability" and "powerfulness." However, these robots are heavy and unsuitable for fragile objects and human interactions. In contrast, soft robotics, which utilizes flexible components, offers a promising approach to addressing these challenges. Numerous soft robots have been developed for applications in various fields, including human assistive devices such as rehabilitation equipment [1], [2] and exosuits [3], [4]; medical devices for procedures such as endoscopic [5] and minimally invasive surgeries [6], [7]; and industrial equipment such as soft robotic hands [8], [9].

Pneumatic artificial muscles are a type of soft actuator, also familiar as McKibben artificial muscles, and have been studied in both analytical and experimental aspects [10], [11]. While axial movement pneumatic artificial muscle has been extensively explored, there has been relatively limited research on developing straightforward pneumatic actuators for twisting motion [12], [13]. To increase the applicability of soft robots, actuators that can achieve a greater variety of motions are needed. Therefore, this study specifically focuses on actuators that enable twisting motions.

In previous research, soft power-assistive wear that can support forearm twisting (inward and outward rotation) [14], a tilting mirror platform [15], mobile robots [16], and a trunk-like manipulator [17] have been developed by using twisting artificial muscles. Table I summarizes recent examples of pneumatic twisting artificial muscles. They can be classified into two types based on the material and twisting principle: those that use spiral-shaped rigid bodies to constrain an elastic body [14], [16], [17], [18], [19], [20], and those that have asymmetrical air chambers [15], [21]. These pneumatic twisting artificial muscles can also be categorized based on three fabrication methods: molding and soft lithography [15], [16], [18], [19], [21], using spiral non-stretchable materials to constrain linear motion artificial muscles [14], [17], and 3D printing [20]. Although molding and soft lithography are the most commonly used methods, they require additional steps such as mold making and rubber curing, which can increase the number of manufacturing steps and prolong production time. When pneumatic artificial muscles are constrained by spiral-shaped rigid bodies, productivity is poor because manual labor is required. Although 3D printing has addressed some of the issues associated with the two aforementioned fabrication methods, the composition of the molding ink remains complex, making fabrication challenging.

The McKibben artificial muscle is a pneumatically driven soft actuator comprising a rubber tube and sleeve fibers. In this study, an easy process for fabricating twisting artificial muscles is established by utilizing the braider machine and the water-soluble fibers based on the McKibben artificial muscle. In the braiding process, half of the sleeve fibers of the artificial muscle are substituted with water-soluble fibers However, twisting motion can be realized by removing the water-soluble fibers by placing the muscle in warm water. By changing the direction of the water-soluble fibers, it is possible to produce artificial muscles that twist clockwise or counterclockwise.

The letter is structured as follows: In Section II, we discuss an overview of the twisting artificial muscle and the analytical model. In Section III, we introduce the braiding technology, followed by the fabrication of twisting artificial muscles. In

Manuscript received 2 October 2023; accepted 14 January 2024. Date of publication 31 January 2024; date of current version 22 February 2024. This letter was recommended for publication by Associate Editor J. Sheng and Editor J.P. Desai upon evaluation of the reviewers' comments. The work was supported in part by Grant-in-Aid for JSPS Research Fellowships for Young Scientists under Grant 23KJ1604 and in part by the Grants-in-Aid for Scientific Research under Grant 20K04240 of Japan Society for the Promotion of Sciences. *(Corresponding author: Shuichi Wakimoto.)*

The authors are with the Graduate School of Environment, Life, Natural Science and Technology, Okayama University, Okayama 700–8530, Japan (e-mail: pd339tfj@s.okayama-u.ac.jp; wakimoto@okayama-u.ac.jp; yamaguchi20@okayama-u.ac.jp; kanda-t@okayama-u.ac.jp).

Digital Object Identifier 10.1109/LRA.2024.3360817

TABLE I
SUMMARY OF PNEUMATIC TWISTING ARTIFICIAL MUSCLES

Study	Material of Actuator	Manufacturing Method
Noritsugu *et al.* [14]	Elastic material and non-stretchable material	Rubber artificial muscle restrained by helical fibers
Gorissen *et al.* [15]	Elastic material	Soft lithography techniques
Connolly *et al.* [16]	Elastic material and non-stretchable material	Casting technologies
Guan *et al.* [17]	Elastic material and non-stretchable material	McKibben artificial muscle restrained by one helical plate
Lee *et al.* [18]	Elastic material and non-stretchable material	Casting technologies
Martinez *et al.* [19]	Elastic material and non-stretchable material	Casting technologies
Yang *et al.* [21]	Elastic material	Casting technologies
Schaffner *et al.* [20]	Elastic material and non-stretchable material	3D printing (Direct ink writing)

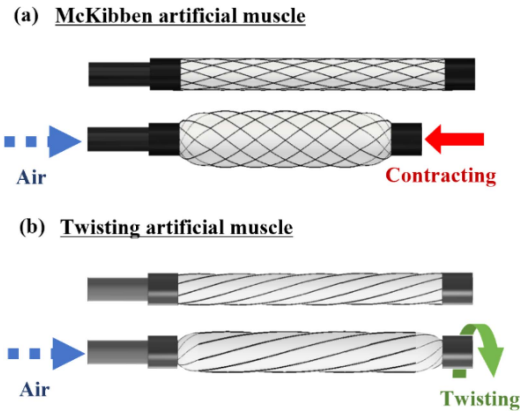

Fig. 1. Images of artificial muscles.

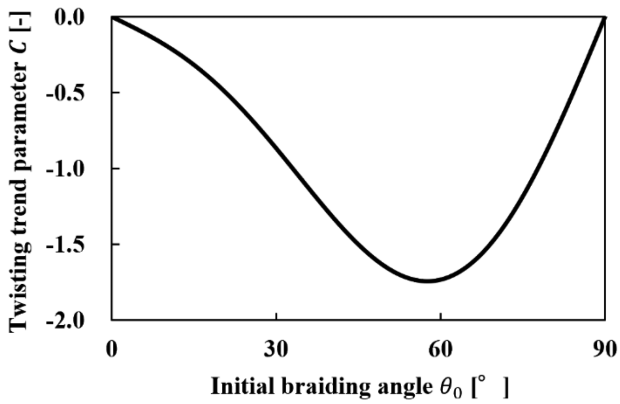

Fig. 2. Relationship between the initial braiding angle θ_0 and the twisting trend parameter C.

Section IV, we evaluate the fabricated twisting artificial muscles and compare with the analytical model. Finally, the conclusions and future work are presented in Section V.

II. TWISTING ARTIFICIAL MUSCLES

A. Overview

The McKibben artificial muscle is a pneumatic actuator developed in the 1950s [11]. It has a simple structure consisting of a rubber tube that encloses air and a sleeve fiber that covers it. It has advantageous features such as good human compatibility and a high output-weight ratio. Therefore, they are used as actuators for robots that work in environments close to humans, prosthetic hands [22], assist suits [4], and rehabilitation devices [21] that support humans; moreover, they are applied in various fields.

Fig. 1(a) illustrates a model of the McKibben artificial muscle. When air pressure is applied to the rubber tube, it starts to expand, and the sleeve fibers work like in a pantograph mechanism. This action causes the artificial muscle to expand radially and contract axially. Also, a twisting motion can be achieved using spiral fibers to constrain the flexible pneumatic chambers [16]. The sleeve of the McKibben artificial muscle is composed of fibers that constrain both clockwise and counterclockwise directions. Therefore, removing half of the sleeve fibers (clockwise or counterclockwise) may enable a twisting motion. Therefore, in this study, we developed a novel fabrication process for twisting artificial muscles by replacing half of the sleeve fibers in the McKibben artificial muscle with water-soluble fibers and subsequently removing these water-soluble fibers to enable twisting motion.

B. Analytical Model

To understand the parameters influencing the operation of twisting artificial muscles, an approximate model is derived for the twist angle of artificial muscles. Twisting artificial muscles are composed of a thin-walled rubber tube and restrained fibers arranged parallel to it. By simplifying this structure as similar to fiber-reinforced composite materials [20], refer to the derivation method of Schaffner et al., the twist angle α of twisting artificial muscles can be expressed by (1). The derivation is discussed in the APPENDIX.

$$\alpha = \frac{pL}{2tE_2} C, \tag{1}$$

$$C = \left(-5\sin^3\theta_0\cos\theta_0 - \sin\theta_0\cos^3\theta_0\right) . \tag{2}$$

where θ_0 is the initial braiding angle between the restrained fiber and the horizontal direction (hereafter, the initial braiding angle), p is the applied pressure, L is the length of the artificial muscle, and E_2 and t are the Young's modulus and wall thickness, respectively, of the used rubber tube. Equation (1) shows that the twist angle depends on the braiding angle θ_0 when the properties

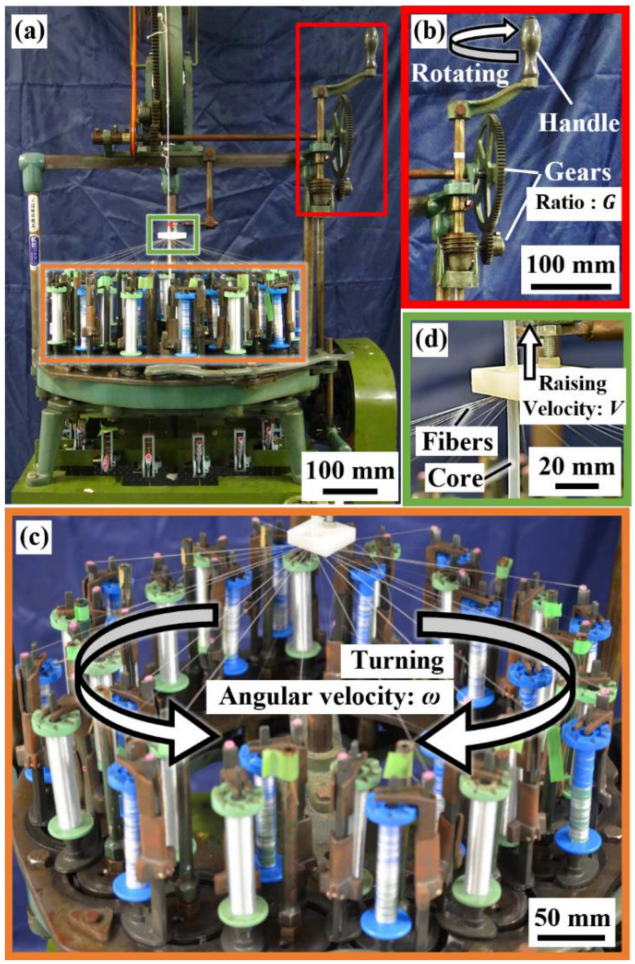

Fig. 3. Braider machine: (a) Appearance; (b) handle and gears; (c) bobbins; and (d) gathering point of the fibers.

of the rubber tubing used for the artificial muscle, the length of the artificial muscle, and the air pressure application conditions are the same. We also describe the trigonometric term C as the twisting trend parameter. The relationship between θ_0 and C is shown in Fig. 2.

Fig. 2 shows that C is less than 0 for the initial braiding angle θ_0 between 0 and 90°. This indicates that the composite material extends in the -y direction (see Fig. 9) and the tip of the artificial muscle turns toward the front as shown in Fig. 1(b). In other words, the artificial muscle twists in the opposite direction when the fiber direction is reversed and the initial braiding angle is negative. Additionally, the twist angle is larger when the initial braiding angle of the artificial muscle is set as approximately 58°.

III. Fabricating Process

A. Braiding Technology

In this study, we used the braider machine, a machine used to manufacture braided strings, to fabricate artificial muscles. Fig. 3(a) shows the braider machine used in this study. The machine is driven by either manually rotating the handle, as shown in Fig. 3(b), or using an electric motor. The braider

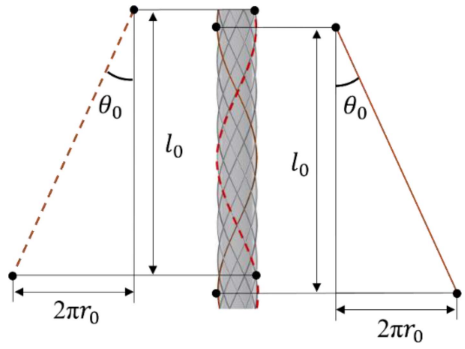

Fig. 4. Model of one pitch of braided fibers.

machine used in this study contained 32 bobbins, as shown in Fig. 3(c). Half of the bobbins (shown in green) rotated clockwise, and the other half (blue) rotated counterclockwise, enabling the braiding of multiple fibers by crossing them alternately to fabricate a braided string. In addition, the fiber material wound around the bobbins can change.

As shown in Fig. 3(d), by attaching a silicone tube to the gathering point of the fibers and pulling it up during braiding, the tube can be covered with evenly braided sleeves of fibers. An acrylic rod is inserted into the tube to maintain its shape, preventing it from deformation by the squeezing force of the fibers.

By adjusting the gear shown in Fig. 3(b), the pulling speed can be changed and the initial braiding angle θ_0 arbitrarily adjusted. The initial braiding angle θ_0 is an important parameter that determines the motion of the twisting artificial muscle. To fabricate the twisting artificial muscle with the initial braiding angle θ_0 that matches the desired specifications, the relationship between the initial braiding angle θ_0 and the gear ratio G of the two gears shown in Fig. 3(b) is derived [24].

The sleeve fibers were arranged in a helical pattern around the silicone tube. An unfolded diagram of one pitch at an initial braiding angle θ_0 is shown in Fig. 4. The directions of the solid red line and the dashed line shown in Fig. 4 are different. If we define the initial length of one pitch when the sleeve fibers of the artificial muscle make one radial turn as l_0 and the radius of the artificial muscle cross section as r_0, the initial braiding angle θ_0 can be defined as follows:

$$\theta_0 = \pm \tan^{-1}\left(\frac{2\pi r_0}{l_0}\right). \tag{3}$$

Defining the speed at which the braider machine pulls up the silicone tube as V and the time it takes for the fiber coming from the bobbin to make one revolution around the tube as t_c, the initial length of one pitch l_0, can be expressed by the following equation:

$$l_0 = Vt_c. \tag{4}$$

If the angular velocity at which the fibers wind around the tube is ω, (5) is obtained.

$$t_c = \frac{2\pi r_0}{\omega}. \tag{5}$$

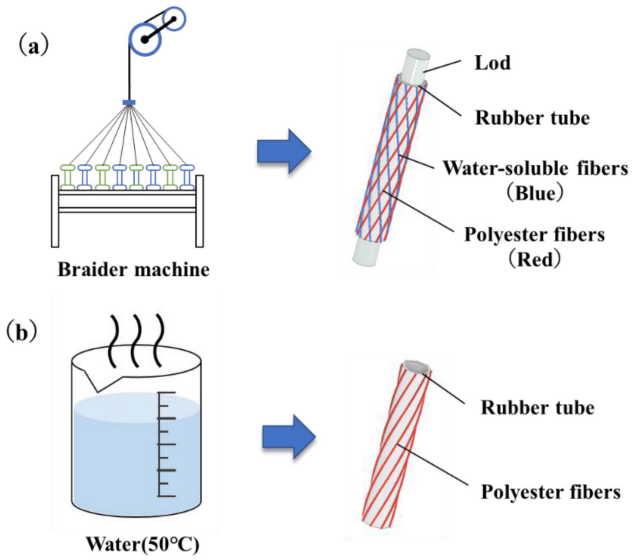

Fig. 5. Fabricating process of the developed twisting artificial muscles: (a) Braiding fibers using the braider machine; (b) dissolving water-soluble fibers in warm water.

Substituting (3) into (4) and (5), the initial braiding angle θ_0 is obtained using (6).

$$\theta_0 = \pm \tan^{-1}\left(\frac{\omega}{V} r_0\right). \tag{6}$$

Assuming that the inner diameter of the tube remains constant, the initial braiding angle is determined by the ratio of the angular velocity ω to the pulling speed V. If we define the pulling speed at gear ratio $G = 1$ as v, (7) is obtained.

$$V = Gv. \tag{7}$$

By substituting (6) into (7), the initial braiding angle θ_0 can be found using (8).

$$\theta_0 = \pm \tan^{-1}\left(\frac{\omega}{v}\,\frac{r_0}{G}\right). \tag{8}$$

Here, the angular velocity ω and the pulling speed v are constant, and the radius r_0 of the artificial muscle is known; hence, the gear ratio G for producing an artificial muscle with any initial braiding angle θ_0 can be obtained. ω/v was found to be 0.16 mm^{-1} on the braider machine used in this study. Therefore, it is possible to determine the twist angle α from the gear ratio G by using (1) and (8).

B. Fabrication of Twisting Artificial Muscles

The two main processes involved in fabrication are sleeve production and the removal of water-soluble fibers using warm water.

The sleeve is composed of a combination of water-soluble and polyester fibers, as shown in Fig. 5(a). Water-soluble fiber is a type of vinyl-type fiber that dissolves in water at a temperature of 30 °C or higher. An acrylic rod is inserted into the rubber tube to prevent its deformation due to the tightening force of the fibers. After braiding the fibers, the rod is pulled out, and a terminal treatment is performed to enable the application of air

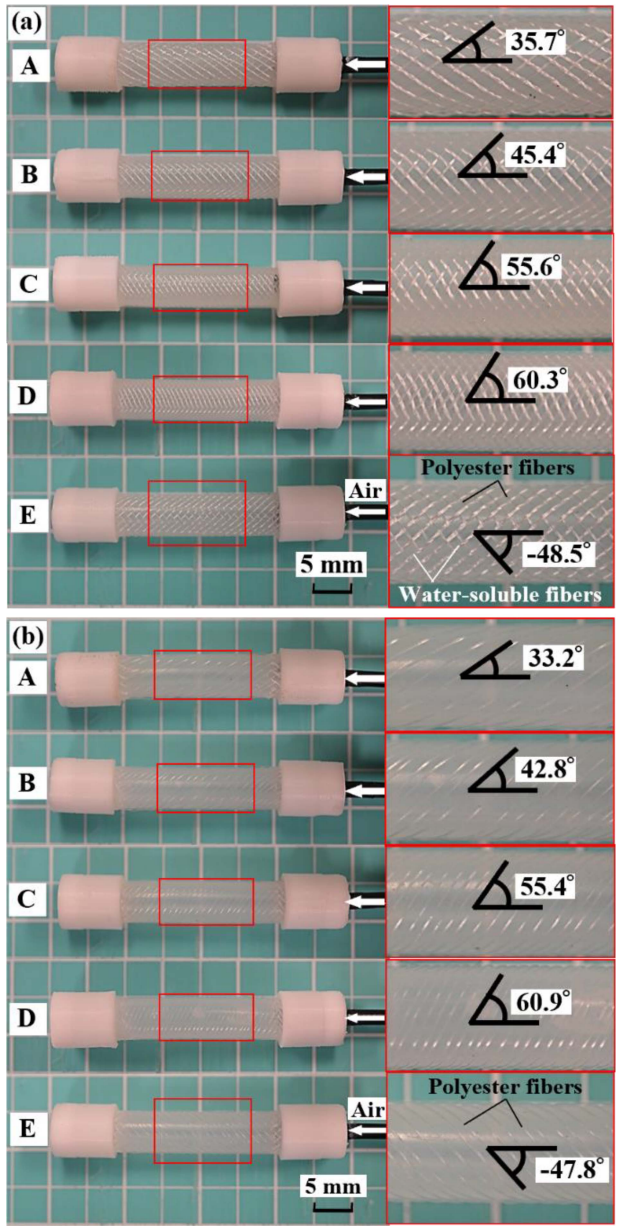

Fig. 6. Appearance of twisting artificial muscles: (a) Before removing water-soluble fibers (upper part); (b) after removing water-soluble fibers (lower part). Note that the angles shown in the figure are the braiding angles of polyester fibers.

pressure, resulting in the production of an artificial muscle. The artificial muscle is then placed in warm water for 60 s with shaking to dissolve the water-soluble fibers and allow for twisting movements when air pressure is applied. All the materials used in the proposed fabrication process are commercially available. Compared to methods such as molding or 3D printing, neither time is expended on liquid rubber curing nor effort is needed to prepare printing ink. Additionally, sleeves are produced using machinery, ensuring efficient fabrication.

Five twisting artificial muscles with different initial braiding angles were fabricated. Fig. 6 shows the twisting artificial muscles fabricated, the artificial muscle before removing the water-soluble fibers is shown in the upper part, and after treatment is

TABLE II
PARAMETERS OF TWISTING ARTIFICIAL MUSCLES

Sample name	Gear ratio G	Braiding angle θ_0 (Theoretical)	Braiding angle θ_0 (Before)	Braiding angle θ_0 (After)
A	0.550	36.0°	35.7°	33.2°
B	0.400	45.0°	45.4°	42.8°
C	0.280	55.0°	55.6°	55.4°
D	0.227	60.4°	60.3°	60.9°
E	0.360	-48.0°	-48.5°	-47.8°

shown in the lower part. As can be seen from the photo in the upper part, the water-soluble fibers and transparent polyester fibers intersect. As shown in the lower part, the water-soluble fibers were removed, and only the transparent polyester fibers restrained the tube.

When fabricating twisting artificial muscles A, B, C and D, the fibers used for the bobbin rotating clockwise (green, shown in Fig. 3(c)) are water-soluble fibers, whereas the fibers used for the remaining bobbin (blue) are polyester fibers. In addition, artificial muscle E was fabricated to investigate the motion of the twisting artificial muscle when the initial braiding angle was negative. When fabricating twisting artificial muscle E, the fibers used for the bobbin rotating clockwise (green) are polyester fibers, whereas the fibers used for the remaining bobbin (blue) are water-soluble fibers.

Additionally, the length of the drivable part (other than the white end parts on the left and right sides of the artificial muscle shown in Fig. 6) of all artificial muscles is 20 mm. The thickness and outer diameter of the rubber tube (TUBS-4-5-N-10, Misumi) used in the fabrication are 0.5 mm and 5 mm, respectively. Tensile test specimens of the rubber tubing were fabricated and tensile tests were conducted, Young's modulus of the tubing was 2.8 MPa.

Table II lists the gear ratios used in the fabrication of each artificial muscle, the theoretical initial braiding angle of polyester fibers calculated using (8), and the actual initial braiding angles of polyester fibers before and after dissolving the water-soluble fibers. Comparing the theoretical initial braiding angle with the actual braiding angle before dissolving the water-soluble fibers, the deviation in the braiding angle for all artificial muscles remained below 1°. Furthermore, when comparing the actual braiding angles before and after dissolving, artificial muscles A and B exhibited a deviation of approximately 3°. The reason for this is that in cases of smaller braiding angles, gaps are formed between the fibers and the tube. Before dissolution, fibers with different orientations exert pressure on each other, maintaining the braiding angle through static friction. However, after dissolution, this static friction force disappears, causing the fibers to attempt to return to their original straight state from the spiral shape, resulting in a smaller braiding angle.

In addition, if the initial braiding angle is too small, the fibers restraining the rubber tube become sparse, causing durability concerns. We experimentally confirmed that the braider machine cannot fabricate twisting artificial muscles with an initial braiding angle of 60.9° or greater. Therefore, the range of initial braiding angles of twisting artificial muscles that can be fabricated using this fabrication process should be from approximately 33.2° to 60.9° (-60.9° to -33.2° is also possible considering the axial symmetry of the fibers). Based on the above observations, it was confirmed that by using a braiding machine and adjusting the gear ratio, it is possible to fabricate twisting artificial muscles with any desired initial braiding angle from approximately 33.2° to 60.9°.

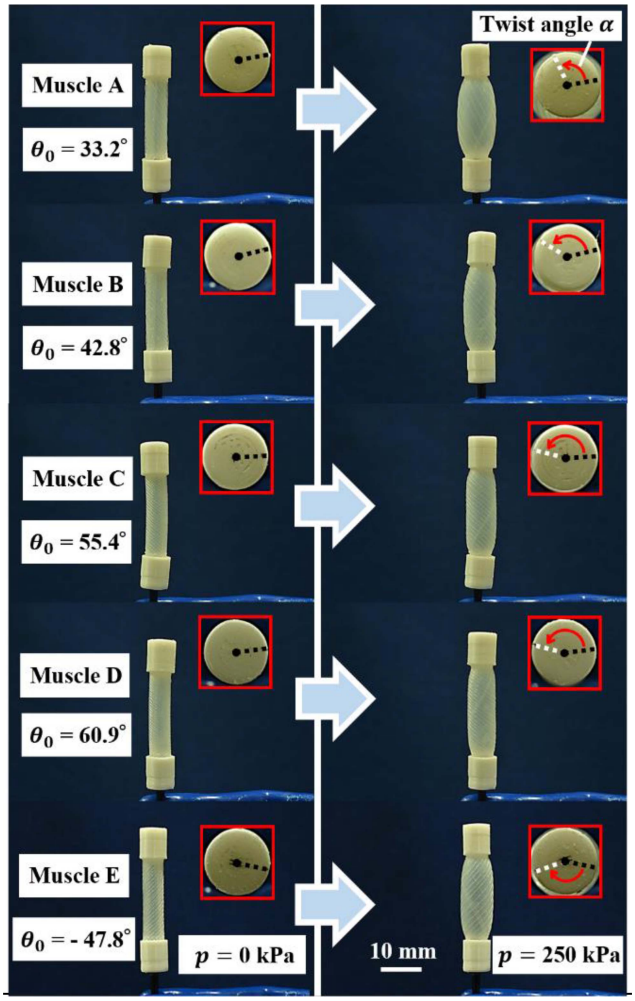

Fig. 7. Twisting artificial muscles before (left side) and after (right side) pneumatic application.

IV. RESULTS AND DISCUSSION

Fig. 7 shows the appearance of the fabricated twisting artificial muscles before and after the application of air pressure. The view from above is shown in the top-right corner of each photo. Considering Fig. 7, the artificial muscles (A, B, C, and D) with positive braiding angle rotate counterclockwise. The artificial muscle (E) with a negative braiding angle rotates clockwise.

After applying air pressure from $p = 0$ kPa to 250 kPa in increments of 50 kPa to the artificial muscle and then reducing it back to 0 kPa, the twisting characteristics were investigated.

Fig. 8 shows the relationship between air pressure and twist angle of the artificial muscles. The plot shows the actual twist angle for each air pressure value measured using image analysis

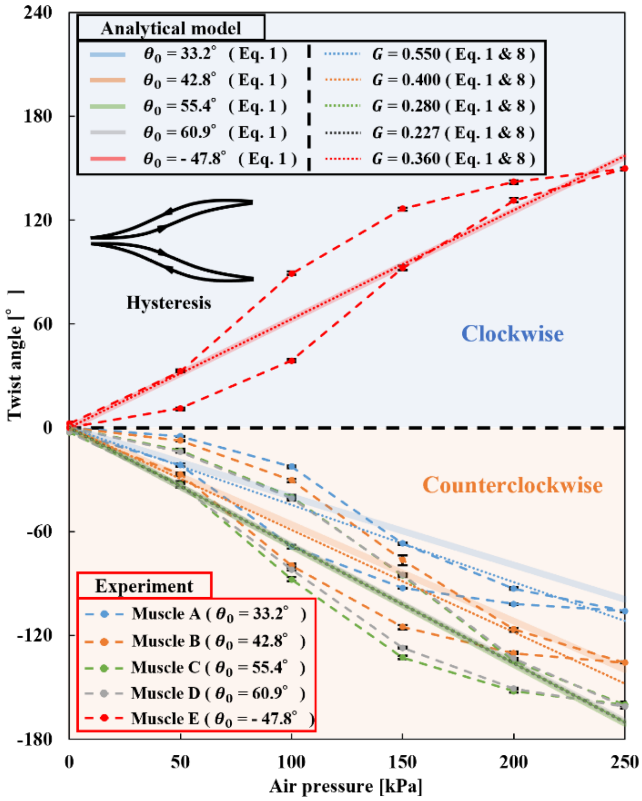

Fig. 8. Relationship between air pressure and twist angle of the artificial muscle.

software. It is observed that the artificial muscle twists with the application of air pressure. In addition, hysteresis was observed in the relationship between the twist angle and the applied pressure on the twisting artificial muscle. This was presumed to be due to the friction between the sleeve fibers and rubber tubes, similar to the hysteresis observed in the contraction ratio relationship with the applied pressure for the McKibben artificial muscles [10], [25].

The maximum twist angles of the twisting artificial muscles fabricated with initial braiding angle between 0 and 58° (muscles A, B, and C) are -105.8°, -136.0°, and -161.2°, respectively; the twisting performance gradually increases. For the artificial muscles with initial braiding angle exceeding 58° (muscle D), the maximum torsion angle is -160.3°, comparable to that of artificial muscle C. Additionally, for artificial muscles with a negative initial braiding angle (muscle E), the maximum twist angle is 150.4°, indicating twisting in the opposite direction. These trends align with the graph depicted in Fig. 2. Furthermore, the light-colored solid lines are the values calculated by substituting the actual braiding angles into (1), and the dotted lines are the values calculated from the gear ratios of each artificial muscle using both (1) and (8). Comparing the actual twist angle (the plot) for each value of air pressure and the values calculated from analytical model, there are slight deviations, but the overall trend is consistent, indicating the usefulness of the models in predicting twisting performance. Evidently, the twisting performance of the artificial muscles can be predicted from the gear ratio.

V. Conclusion

By applying braiding technology and water-soluble fibers, a twisting artificial muscle based on McKibben artificial muscles can be easily fabricated. In addition, by changing the direction of the water-soluble fibers, artificial muscles that twist clockwise or counterclockwise can be produced. We believe that the establishment of such a simple and efficient fabrication process will promote the practical application of artificial muscles.

If this soft actuator manufacturing technology is further developed, it has the potential to create structures with various applications, from biomedical devices such as prosthetic arms and legs that can perfectly replicate human limb movements to soft motion robots that can move in narrow spaces in complex environments, such as disaster sites.

In the future, we will focus on establishing a simple fabricating process for artificial muscles that can curve. We intend to create curving artificial muscles and twisting artificial muscles and then combine these two types of artificial muscles to develop an endoscope with two degrees of freedom. Furthermore, by developing the fabrication process established in this study and using the cores not as rubber tubes but as artificial muscles, we aim to fabricate artificial muscles that can perform more complex movements. For example, when using a curving artificial muscle as a core, twisting while curving is possible. This will further increase the variety of soft actuator movements and meet various needs.

Appendix
Derivation of (1)

When deploying a twisting artificial muscle, it assumes a configuration as that shown in Fig. 9.

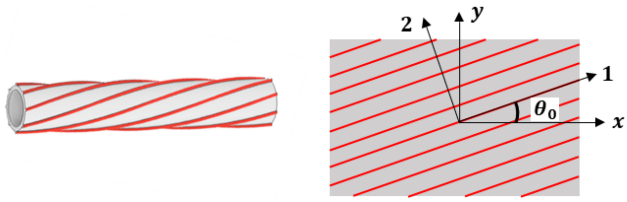

Fig. 9. Model and deployed view of the twisting artificial muscle.

The behavior in the direction of the fibers is governed by the properties of the restrained fibers, while the behavior in the direction perpendicular to the fibers is determined by the properties of the rubber tube. Assuming this, the strains ε_1 and ε_2 in the 1 and 2 directions, respectively, as well as the shear strain γ_{12}, are expressed as follows:

$$\begin{pmatrix} \varepsilon_1 \\ \varepsilon_2 \\ \gamma_{12} \end{pmatrix} = \begin{pmatrix} S_{11} & S_{12} & 0 \\ S_{12} & S_{22} & 0 \\ 0 & 0 & S_{66} \end{pmatrix} \begin{pmatrix} \sigma_1 \\ \sigma_2 \\ \tau_{12} \end{pmatrix} = \begin{pmatrix} \frac{1}{E_1} & -\frac{v_{12}}{E_1} & 0 \\ -\frac{v_{12}}{E_1} & \frac{1}{E_2} & 0 \\ 0 & 0 & \frac{1}{G_{12}} \end{pmatrix} \begin{pmatrix} \sigma_1 \\ \sigma_2 \\ \tau_{12} \end{pmatrix}. \quad \text{(A.1)}$$

Here, σ_1, σ_2, and τ_{12} represent the stresses in the 1 and 2 directions and the shear stress, respectively. E_1 and E_2 are the Young's moduli of the fibers and rubber, respectively, while v_{12} is the Poisson's ratio of the composite material; moreover, G_{12} is the shear modulus. Additionally, the strains ε_x and ε_y in the x and y directions, respectively, as well as the shear strain γ_{xy}, are expressed as follows:

$$\begin{pmatrix} \varepsilon_x \\ \varepsilon_y \\ \gamma_{xy} \end{pmatrix} = \begin{pmatrix} \overline{S_{11}} & \overline{S_{12}} & \overline{S_{16}} \\ \overline{S_{12}} & \overline{S_{22}} & \overline{S_{26}} \\ \overline{S_{16}} & \overline{S_{26}} & \overline{S_{66}} \end{pmatrix} \begin{pmatrix} \sigma_x \\ \sigma_y \\ \tau_{xy} \end{pmatrix}. \tag{A.2}$$

Here, the components $\overline{S_{16}}$ and $\overline{S_{26}}$ of the matrix in (A.2) can be expressed in terms of the components of the matrix in (A.1) and the angle between fiber and 1 direction θ_0 (in the case of twisting artificial muscle: the braiding angle) [26].

$$\begin{aligned} \overline{S_{16}} = {} & (2S_{11} - 2S_{12} - S_{66})\ \sin\theta_0\cos^3\theta_0 \\ & - (2S_{22} - 2S_{12} - S_{66})\sin^3\theta_0\cos\theta_0, \end{aligned} \tag{A.3}$$

$$\begin{aligned} \overline{S_{26}} = {} & (2S_{11} - 2S_{12} - S_{66})\ \sin^3\theta_0\cos\theta_0 \\ & - (2S_{22} - 2S_{12} - S_{66})\sin\theta_0\cos^3\theta_0. \end{aligned} \tag{A.4}$$

When pressure p is applied to the inner surface of a thin-walled cylinder, the axial stress σ_x and circumferential stress σ_y are given by the following equations:

$$\sigma_x = \frac{pD}{4t}, \tag{A.5}$$

$$\sigma_y = \frac{pD}{2t}. \tag{A.6}$$

Here, D and t represent the outer diameter and thickness of the rubber tube, respectively. Substituting (A.2) into (A.5) and (A.6), we get the following expression for shear strain γ_{xy}.

$$\gamma_{xy} = \overline{S_{16}}\,\sigma_x + \overline{S_{26}}\,\sigma_y = \frac{pD}{4t}\left(\overline{S_{16}} + 2\overline{S_{26}}\right). \tag{A.7}$$

Now, substituting (A.3) and (A.4) into (A.7), (A.8) is obtained.

$$\begin{aligned} \gamma_{xy} = {} & \frac{pD}{4t}\left(\frac{4}{E_1} + \frac{2v_{12}}{E_1} - \frac{2}{E_2} - \frac{1}{G_{12}}\right)\sin^3\theta_0\cos\theta_0 \\ & + \frac{pD}{4t}\left(\frac{2}{E_1} - \frac{2v_{12}}{E_1} - \frac{4}{E_2} + \frac{1}{G_{12}}\right)\sin\theta_0\cos^3\theta_0. \end{aligned} \tag{A.8}$$

The shear modulus G_{12} can be calculated based on the Young's modulus E_{45} and the Poisson's ratio v_{45} in the direction of the fibers and at 45°. However, for the sake of simplicity in the model, it is assumed that the behavior in the direction of the fibers and at 45° is determined by the properties of the rubber; accordingly, (A.9) is obtained.

$$\frac{1}{G_{12}} = \frac{2\left(1 + v_{45}\right)}{E_{45}} \fallingdotseq \frac{2\left(1 + v_{12}\right)}{E_2}. \tag{A.9}$$

Furthermore, since the primary material in the composite is rubber, the Poisson's ratio of the composite material is approximated as $v_{12} = 0.5$. Additionally, it is assumed that the Young's modulus of the constrained fibers is extremely high; therefore, $1/E_1 = 0$ is approximated. While these approximations reduce the accuracy of the model, they greatly simplify the strain calculation. Therefore, the shear strain γ_{xy} is as follows.

$$\gamma_{xy} = \frac{pD}{4tE_2}\left(-5\sin^3\theta_0\cos\theta_0 - \sin\theta_0\cos^3\theta_0\right). \tag{A.10}$$

The twisting angle α of the cylinder tip can be calculated from the shear strain γ_{xy}.

$$\alpha = \frac{2L}{D}\gamma_{xy}. \tag{A.11}$$

Here, L represents the length of the artificial muscle. Therefore, the twisting angle α can be calculated using the following equation.

$$\alpha = \frac{pL}{2tE_2}C, \tag{1}$$

$$C = \left(-5\sin^3\theta_0\cos\theta_0 - \sin\theta_0\cos^3\theta_0\right). \tag{2}$$

REFERENCE

[1] P. Polygerinos, Z. Wang, K. C. Galloway, R. J. Wood, and C. J. Walsh, "Soft robotic glove for combined assistance and at-home rehabilitation," *Robot. Auton. Syst.*, vol. 73, pp. 135–143, Nov. 2015, doi: 10.1016/j.robot.2014.08.014.

[2] H. K. Yap et al., "A fully fabric-based bidirectional soft robotic glove for assistance and rehabilitation of hand impaired patients," *IEEE Robot. Automat. Lett.*, vol. 2, no. 3, pp. 1383–1390, Jul. 2017, doi: 10.1109/LRA.2017.2669366.

[3] L. N. Awad et al., "A soft robotic exosuit improves walking in patients after stroke," *Sci. Transl. Med.*, vol. 9, no. 400, Jul. 2017, Art. no. eaai9084, doi: 10.1126/scitranslmed.aai9084.

[4] T. Abe et al., "Fabrication of '18 Weave' muscles and their application to soft power support suit for upper limbs using thin McKibben muscle," *IEEE Robot. Automat. Lett.*, vol. 4, no. 3, pp. 2532–2538, Jul. 2019, doi: 10.1109/LRA.2019.2907433.

[5] B. Gorissen, M. De Volder, and D. Reynaerts, "Chip-on-tip endoscope incorporating a soft robotic pneumatic bending microactuator," *Biomed. Microdevices*, vol. 20, no. 3, Sep. 2018, Art. no. 73, doi: 10.1007/s10544-018-0317-1.

[6] H. Abidi et al., "Highly dexterous 2-module soft robot for intra-organ navigation in minimally invasive surgery," *Int. J. Med. Robot.*, vol. 14, no. 1, Feb. 2018, Art. no. e1875, doi: 10.1002/rcs.1875.

[7] M. Cianchetti et al., "Soft robotics technologies to address shortcomings in today's minimally invasive surgery: The STIFF-FLOP approach," *Soft Robot.*, vol. 1, no. 2, pp. 122–131, Jun. 2014, doi: 10.1089/soro.2014.0001.

[8] C. Tawk, A. Gillett, M. I. Het Panhuis, G. M. Spinks, and G. Alici, "A 3D-printed omni-purpose soft gripper," *IEEE Trans. Robot.*, vol. 35, no. 5, pp. 1268–1275, Oct. 2019, doi: 10.1109/TRO.2019.2924386.

[9] P. Glick, S. A. Suresh, D. Ruffatto, M. Cutkosky, M. T. Tolley, and A. Parness, "A soft robotic gripper with gecko-inspired adhesive," *IEEE Robot. Automat. Lett.*, vol. 3, no. 2, pp. 903–910, Apr. 2018, doi: 10.1109/LRA.2018.2792688.

[10] C. P. Chou and B. Hannaford, "Static and dynamic characteristics of McKibben pneumatic artificial muscles," in *Proc. IEEE Int. Conf. Robot. Automat.*, 1994, vol. 1, pp. 281–286, doi: 10.1109/ROBOT.1994.350977.

[11] B. Tondu, "Modelling of the McKibben artificial muscle: A review," *J. Intell. Mater. Syst. Struct.*, vol. 23, no. 3, pp. 225–253, Feb. 2012, doi: 10.1177/1045389X11435435.

[12] S. Aziz and G. M. Spinks, "Torsional artificial muscles," *Mater. Horiz.*, vol. 7, no. 3, pp. 667–693, 2020, doi: 10.1039/C9MH01441A.

[13] S. Sanan, P. S. Lynn, and S. T. Griffith, "Pneumatic torsional actuators for inflatable robots," *J. Mech. Robot.*, vol. 6, no. 3, Aug. 2014, Art. no. 031003, doi: 10.1115/1.4026629.

[14] T. Noritsugu, "Development of power assist wear driven with pneumatic rubber artificial muscle," *J. Robot. Soc. Jpn.*, vol. 33, no. 4, pp. 222–227, 2015, doi: 10.7210/jrsj.33.222.

[15] B. Gorissen, T. Chishiro, S. Shimomura, D. Reynaerts, M. De Volder, and S. Konishi, "Flexible pneumatic twisting actuators and their application to tilting micromirrors," *Sensors Actuators A: Phys.*, vol. 216, pp. 426–431, Sep. 2014, doi: 10.1016/j.sna.2014.01.015.

[16] F. Connolly, P. Polygerinos, C. J. Walsh, and K. Bertoldi, "Mechanical programming of soft actuators by varying fiber angle," *Soft Robot.*, vol. 2, no. 1, pp. 26–32, Mar. 2015, doi: 10.1089/soro.2015.0001.

[17] Q. Guan, J. Sun, Y. Liu, N. M. Wereley, and J. Leng, "Novel bending and helical extensile/contractile pneumatic artificial muscles inspired by elephant trunk," *Soft Robot.*, vol. 7, no. 5, pp. 597–614, Oct. 2020, doi: 10.1089/soro.2019.0079.

[18] J. Y. Lee, W. B. Kim, W. Y. Choi, and K. J. Cho, "Soft robotic blocks: Introducing SoBL, a fast-build modularized design block," *IEEE Robot. Automat. Mag.*, vol. 23, no. 3, pp. 30–41, Sep. 2016, doi: 10.1109/MRA.2016.2580479.

[19] R. V. Martinez, C. R. Fish, X. Chen, and G. M. Whitesides, "Elastomeric origami: Programmable paper-elastomer composites as pneumatic actuators," *Adv. Funct. Mater.*, vol. 22, no. 7, pp. 1376–1384, Feb. 2012, doi: 10.1002/adfm.201102978.

[20] M. Schaffner, J. A. Faber, L. Pianegonda, P. A. Rühs, F. Coulter, and A. R. Studart, "3D printing of robotic soft actuators with programmable bioinspired architectures," *Nature Commun.*, vol. 9, no. 1, p. 878, Dec. 2018, doi: 10.1038/s41467-018-03216-w.

[21] D. Yang et al., "Buckling of elastomeric beams enables actuation of soft machines," *Adv. Mater.*, vol. 27, no. 41, pp. 6323–6327, Nov. 2015, doi: 10.1002/adma.201503188.

[22] H. Taniguchi et al., "Realistic and highly functional pediatric externally powered prosthetic hand using pneumatic soft actuators," *J. Robot. Mechatronics*, vol. 32, no. 5, pp. 1034–1043, Oct. 2020, doi: 10.20965/jrm.2020.p1034.

[23] S. Koizumi et al., "Soft robotic gloves with thin McKibben muscles for hand assist and rehabilitation," in *Proc. IEEE/SICE Int. Symp. Syst. Integration*, 2020, pp. 93–98, doi: 10.1109/SII46433.2020.9025832.

[24] S. Kogawa, S. Wakimoto, T. Kanda, K. Omura, and K. Ando, "Establishment of fabrication process for smart artificial muscles with the inductance sensor," *Trans. Jpn. Fluid Power Syst. Soc.*, vol. 51, no. 2, pp. 25–31, 2020, doi: 10.5739/jfps.51.25.

[25] T. Vo-Minh, T. Tjahjowidodo, H. Ramon, and H. Van Brussel, "A new approach to modeling hysteresis in a pneumatic artificial muscle using the maxwell-slip model," *IEEE/ASME Trans. Mechatronics*, vol. 16, no. 1, pp. 177–186, Feb. 2011, doi: 10.1109/TMECH.2009.2038373.

[26] A. K. Kaw, *Mechanics of Composite Materials* (Mechanical Engineering Series), vol. 29, 2nd ed. New York, NY, USA: Taylor & Francis, 2006.